# Synaptic integration in layer IV of the ferret striate cortex

J. A. Hirsch

*Laboratory of Neurobiology, Box 138, 1230 York Avenue, New York, NY 10021, USA*

1. Whole-cell patch recordings were made with dye-filled electrodes from layer IV in slices of the ferret striate cortex. Projections from the thalamus and layer VI provide most of the extralaminar input to layer IV. Interactions between these two pathways are thought to play a role in the generation of suppressive non-linearities such as end-inhibition. Thus, synaptic responses evoked by stimulating each pathway individually were compared with those produced by activating both projections together.

2. Spiny stellate cells are the majority population in layer IV and were the most frequently patched neurons ($n = 23$); all fired adapting trains of large, fast action potentials. About half of those tested ($n = 13$) were progressively inhibited by strengthening the stimulus to layer VI, while the rest became more excited. For the former, the response evoked by stimulating both pathways in coincidence was often more hyperpolarizing than would have been predicted by summing the responses to either projection alone ($n = 4$). Hence, the inputs from the thalamus and layer VI are integrated by circuits that can produce strong and non-linear inhibition.

3. Recordings from various basket cells, which are inhibitory, have provided a first view of the suppressive circuits in layer IV ($n = 5$). Two cells were excited by stimulation of both pathways. The remaining three cells were mainly excited by activation of thalamic afferents but were largely inhibited by stimulation of layer VI. Thus, inhibition seen at the level of the spiny stellate cells could result from two mechanisms operating via presynaptic smooth cells: convergent excitation provided by both ascending pathways on the one hand, and a push–pull relationship between pathways on the other.

The neural representation of visual space changes at the first synapse between thalamus and cortex. In carnivores, thalamic neurons have circular, symmetric receptive fields. In contrast, cells in layer IV, the main recipients of geniculocortical input, are oriented and are often tuned to parameters such as length or direction (Hubel & Wiesel, 1962; Dreher, 1972; LeVay, McConnell & Luskin, 1987). A central challenge in visual neuroscience is understanding the means by which the cortical circuitry generates functional properties. The appropriate convergence of thalamic inputs may explain some response features such as orientation specificity (Hubel & Wiesel, 1962; Chapman, Zahs & Stryker, 1991). Accounting for other characteristics including length and directional preference (Hubel & Wiesel, 1962, 1965; Dreher, 1972), however, calls for involvement of the intracortical connections. For example, the main intracortical pathway to layer IV, a dense projection from layer VI, is thought to be involved in creating end-inhibition (McGuire, Hornung, Gilbert & Wiesel, 1984; Bolz & Gilbert, 1986).

This study focused on the synaptic integration of inputs supplied both by layer VI and the thalamus to layer IV. Anatomical studies suggest that these projections have functional differences. The axons from layer VI usually end on dendritic shafts and thus may favour inhibitory neurons, because they lack spines, rather than spiny stellate cells (McGuire *et al.* 1984). By contrast, fibres from the thalamus favour dendritic spines, as do the axons of the spiny stellate cells (McGuire *et al.* 1984; Freund, Martin, Somogyi & Whitteridge, 1985; Saint-Marie & Peters, 1985). In this study, responses to the electrical activation of each pathway were recorded with patch electrodes (Hamill, Marty, Neher, Sakmann & Sigworth, 1981; Blanton, LoTurco & Kriegstein, 1989; Edwards, Konnerth, Sakmann & Takahashi, 1989) from layer IV in slices of the ferret visual cortex. Most recordings were made from spiny stellate cells, the majority population in layer IV, and others were made from different classes of smooth neurons. The results suggest that sets of inputs from the thalamus and layer VI are integrated circuits that generate non-linear inhibition. These circuits may play a role in generating suppressive functional properties such as end-stopping. Some of these findings have been presented in abstract form (Hirsch, 1992).

## METHODS

### Anaesthesia and surgery

Ferrets (0·5–1·5 kg) were first anaesthetized with an intramuscular injection of ketamine (10 mg $kg^{-1}$) after which anaesthesia was maintained with intravenous Pentothal (20 mg $kg^{-1}$; Abbot Laboratories, North Chicago, IL, USA). The ECG and temperature were continually monitored and temperature was controlled with a heating pad. After making a craniotomy and reflecting the dura mater over the occipital cortex in one hemisphere, a block containing area 17 of the visual cortex (~1·5 cm mediolateral by 0·5 cm anteroposterior) was excised and placed in ice-cold artificial cerebrospinal fluid (ACSF). The same procedures of excising the tissue and preparing the slices (see below) were repeated for the second hemisphere. After removing the second block, the animal was killed with an overdose of Pentothal.

### Preparation and maintenance of slices

The pia mater was gently removed from the surface of the excised cortex which had been chilled for several minutes in ice-cold ACSF. The block was then trimmed and mounted with cyanoacrylate glue onto a platform, fitted into the stage of a vibratome, and was bathed in ice cold, oxygenated ACSF. Sagittal slices (200–350 $\mu$m thick) were cut and held in a chamber where they were immersed in oxygenated ASCF at 25–30 °C for 2–28 h.

For recording, a slice was submerged in a glass-bottomed chamber with a volume of 0·4 ml and was held stable by a weighted nylon net. The ASCF, warmed to 34–35 °C, flowed through the chamber at a rate of ~0·5 ml $min^{-1}$. The chamber was illuminated from below. It was viewed from above with a dissecting microscope to facilitate the placement of the stimulating and recording electrodes. The white matter and layers IV and VI appeared as opaque bands while the remaining regions of the tissue were translucent.

### Recording and stimulation *in vitro*

Patch electrodes were made from thin-walled borosilicate capillary glass, 1·2 mm o.d., with a resistance of $\leqslant$15 M$\Omega$. Seals between the electrode and the cell membrane were made using the procedure described by Blanton *et al.* (1989). Current and voltage were monitored and delivered with a patch amplifier, outfitted with a headstage designed for whole-cell recording. Recordings were displayed on an oscilloscope and computer terminal, and stored on hard disk and videotape. Resting potentials and input resistances were usually measured from voltage-clamp recordings obtained in the first few minutes after the seal was made; series resistances were uncompensated.

Electrical stimuli were shocks ranging from 1 to 100 V and lasting from 50 to 150 $\mu$s. These were delivered at 0·1 Hz through two sharpened, insulated tungsten wires with a tip separation of ~50 $\mu$m, or occasionally, through a bipolar concentric or a monopolar electrode. In some instances, stimuli were delivered rapidly, at 10–40 Hz, to exhaust synaptic transmission. Stimulus artifacts were reduced off-line.

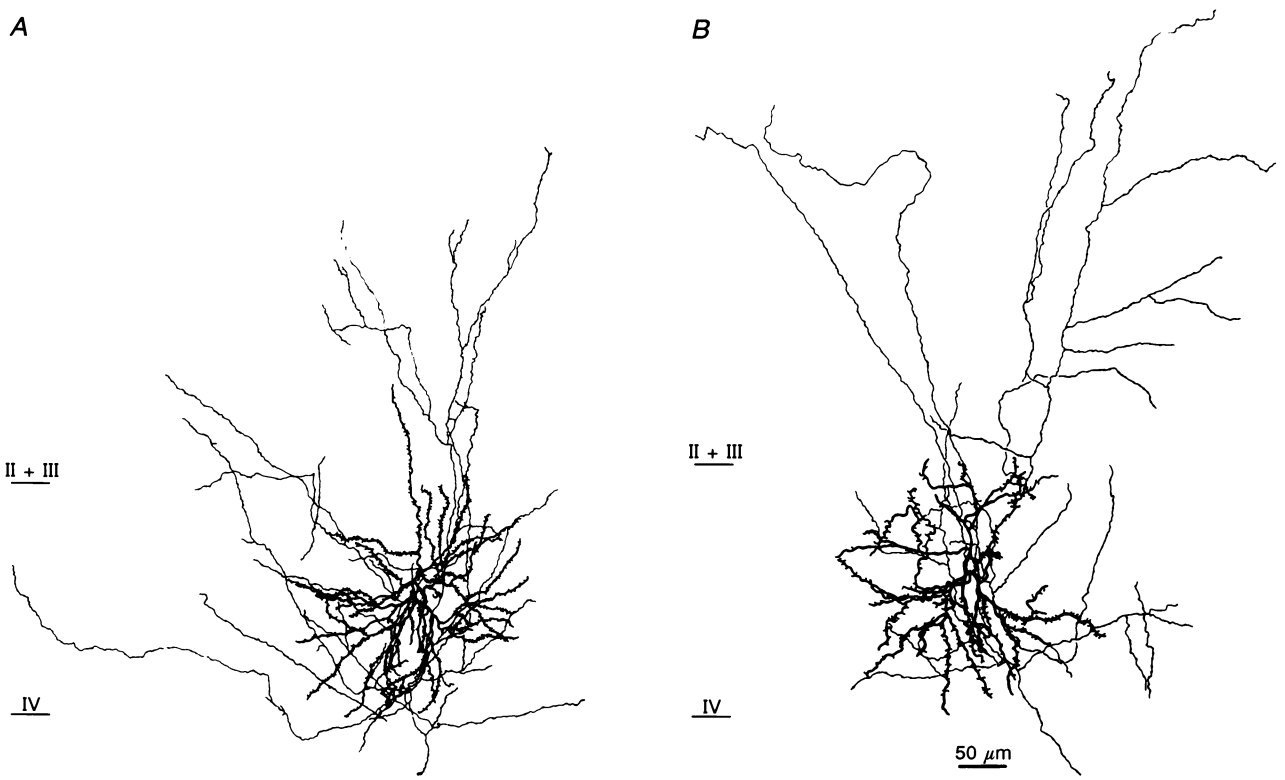


**Figure 1. Intracellularly labelled spiny stellate neurons**

These examples represent two ends of the continuum of this morphological class. The dendritic arbor of the cell in *A* has a round soma and lacks a clear-cut primary apical dendrite. The soma of the cell in *B* is pyramidally shaped and bears a process resembling an apical dendrite; nonetheless, its dendritic arbor is circular, symmetrical and confined to layer IV.

### GABA application

Pipettes with tip openings of 2–5 mm were filled with a solution of 40 mM GABA in ASCF. This solution was delivered to the tissue by applying pressure pulses (40 lbf $in^{-2}$, for 30–100 ms) to the back of the pipette.

### Solutions

The standard ACSF contained (mM): NaCl, 125; KCl, 5; $NaHCO_3$, 26; $CaCl_2$, 2·4; $MgCl_2$, 1·3; and dextrose, 10. It was saturated with 95% $O_2$–5% $CO_2$ and adjusted to pH 7·4. Patch pipettes were filled with an internal solution (IS1) usually composed of (mM): potassium methanesulphonate, 120; NaCl, 5; $CaCl_2$, 1; $MgCl_2$, 1; EGTA, 5; GTP, 0·2; ATP, 2; Hepes, 10–40; biocytin or neurobiotin, 1%; pH 7·3, 280 mosmol $l^{-1}$ (adjusted with sucrose). A little more than midway through the project a switch was made to IS2. This had a composition similar to IS1, except that gluconate was substituted for the methanesulphonate, EGTA was increased to 11 mM, and Hepes was increased to 40 mM. On rare occasions $K^+$ was replaced by $Cs^+$. None of the results discussed here depended on the type of IS used.

### Histology

The tissue containing biocytin-labelled cells was processed using a modification of the technique described in Horikawa & Armstrong (1988). Briefly, slices were fixed overnight in 4% paraformaldehyde, cut into 70–100 $\mu$m sections with a freezing microtome and rinsed twice with phosphate-buffered saline (PBS). The sections were then incubated for 15 min in 0·3% hydrogen peroxide, rinsed 3 times in PBS and then incubated for 45 min in PBS, containing 0·25% Triton X-100 and 2% bovine serum albumin (BSA). After rinsing in PBS with 2% BSA they were incubated in ABC (avidin–biotin complex) reagent (Vector Laboratories, Burlingame, CA, USA) for 2–3 h at room temperature or overnight at 4 °C. The tissue was then washed in PBS, 3 times, each for 15 min, and incubated for 30 min in 0·05% diaminobenzidine (DAB) in PBS. Hydrogen peroxide (0·3%) was added at a ratio of 1:100 to the DAB solution and about 15 min later the sections were rinsed 3 times in PBS. Finally, the sections were mounted, dehydrated and coverslips added. The tissue was counterstained with Cresyl Violet if the background label was insufficient to reveal the cortical laminae. Neurones were reconstructed with a drawing tube attached to a microscope.

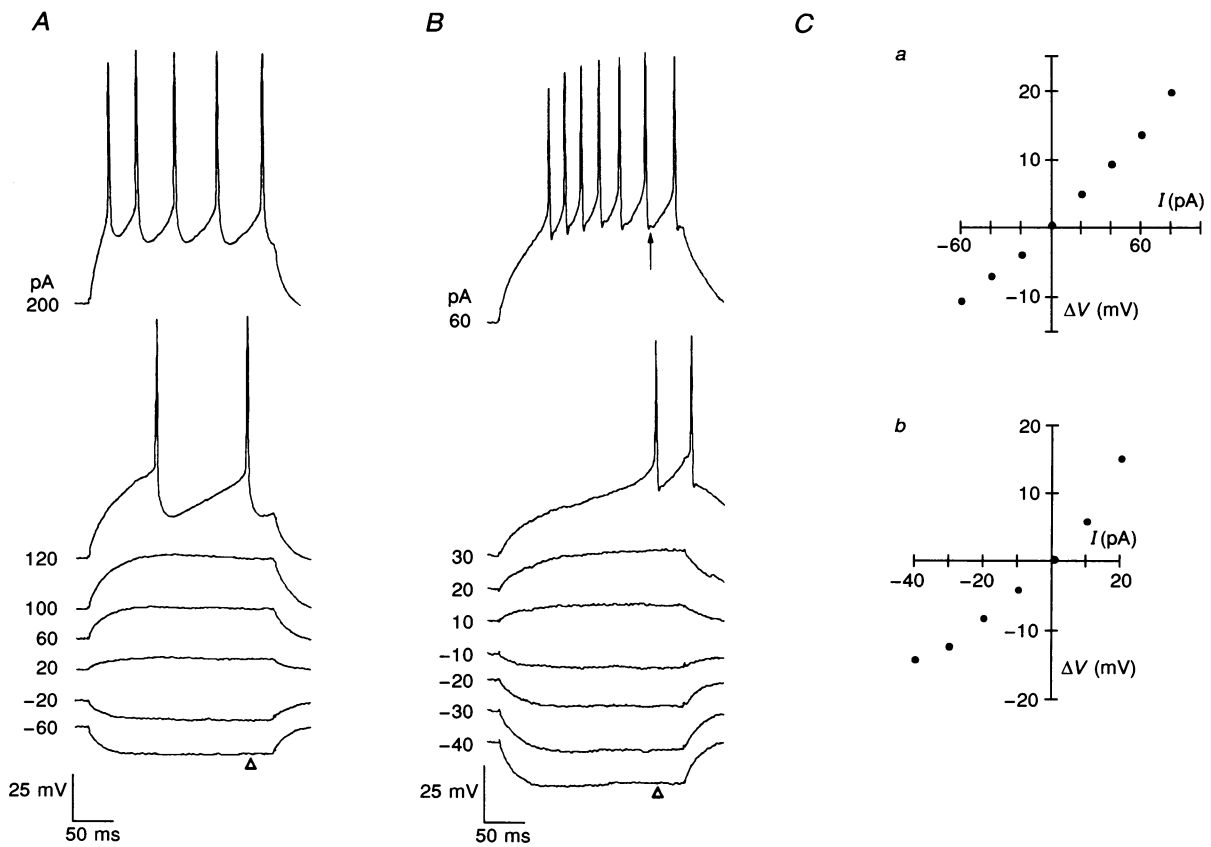


**Figure 2. Electrical properties of spiny stellate cells**

The responses of two neurons to current pulses of various amplitudes are pictured in *A* and *B*. Both cells fired in trains of large regular action potentials but distinct after-depolarizations were evident only in the right-hand traces in *B* (arrow). For the two cells in *A* and *B*, the voltage changes produced by the pulses, at the time point indicated by the arrowhead, are plotted in *Ca* and *Cb*, respectively. Note that for both cells the slope of the curve is steeper above than below the origin. For the cell in *A*, the membrane potential was −59 mV and the input resistance was 230 MΩ. For the cell in *B*, spontaneous firing was subdued by weak continuous hyperpolarization, the resting potential was −60 mV and the input resistance was 450 MΩ.

## RESULTS

Twenty-one ferrets were used for the experiments. The animals ranged in age from 2 to 6 months old; the critical period in ferret has largely ended by the eighth week (Chapman & Stryker, 1993). The neurons shown in Fig. 1 are representative of the major class of neuron included in this study. Cells were identified as spiny stellate using morphological criteria developed in studies of the cat and monkey (Lorente de Nó, 1944; Lund, Henry, Macqueen & Harvey, 1979). The criteria are the lack of a prominent apical dendrite reaching into the superficial layers, and dendrites of roughly equal length. As in other species, spiny stellate cells represented a continuum from distinctly radial and stellate (Fig. 1*A*) to subtly pyramidal (Fig. 1*B*). Axonal arbors principally supplied layers IV, and II + III. The population of cells was too small to assay for physiological trends that paralleled cell size or intralaminar tier.

### Firing properties of spiny cells

For twenty-three morphologically identified spiny stellate cells, the resting potential was −60·1 ± 5·8 mV (mean ± S.D.) and the input resistance, 263 ± 113 MΩ. Every spiny stellate cell identified in the study fired large fast action potentials, the rate of which adapted over time. Input resistance, threshold for firing and resting potential were monitored throughout the recording session and only stable cells were included in the study. The responses of two spiny stellate cells to an injection of current are shown in Fig. 2, representing the range of firing patterns observed. The clearest-cut difference among cells was seen in the shape of the 'undershoots'. The action potentials shown in Fig. 2*B* were followed by multiphasic undershoots that comprised a distinct after-depolarization ($n = 13$, 8 with IS1 and 5 with IS2). No such complex waveforms were apparent in other cells like that shown in Fig. 2*A* ($n = 6$, 4 with IS1 and 2 with IS2). Four cells were recorded in voltage clamp only; in this mode the shape of the undershoot cannot be seen.

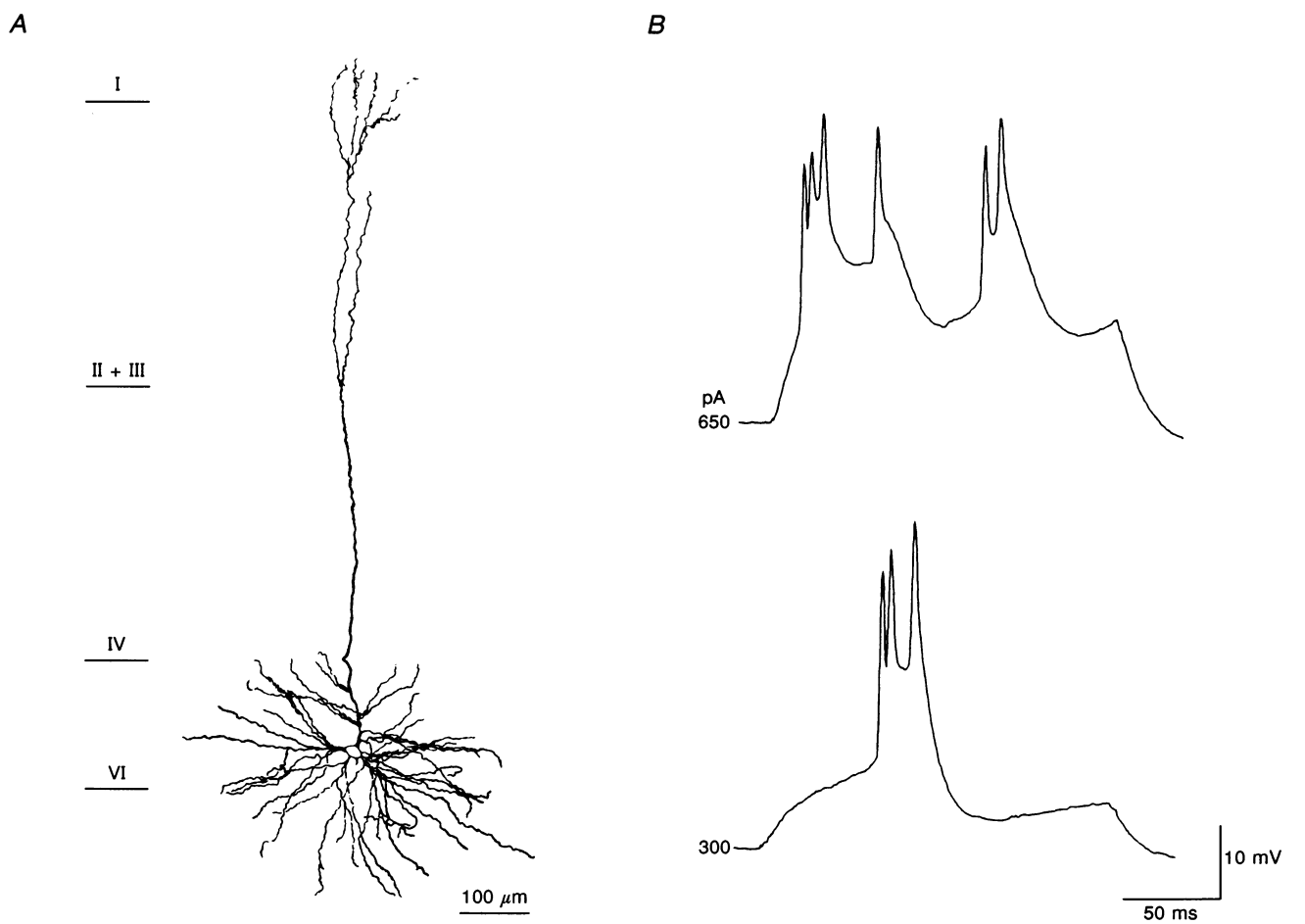


**Figure 3. Bursting responses in layer IV were recorded from the apical dendrites of lower layer pyramids**

The cell pictured in *A* was labelled during a recording made in layer IV. Its responses to pulses of current included bursts of broad, variously sized action potentials (*B*). The resting potential was −57 mV and the input resistance was 200 MΩ.

The plots shown in Fig. 2*Ca* and *b* are the voltage–current relationships measured at the times indicated by the arrowheads in Fig. 2*A* and *B*, respectively. As for all spiny stellate cells sampled, the curves were non-linear, with the slope steeper at voltages close to the threshold for firing. For the cell in Fig. 2*A*, the ratio of the slope above the origin to that below was 1·3; for the cell in Fig. 2*B* this value was 2·0. Slopes were calculated by least-squares regression analysis.

Occasionally, cells that fired bursts of action potentials were patched in layer IV. In these instances, subsequent histology revealed that the recordings had been made from the apical dendrites of pyramids with somas in layers V or VI. Figure 3*B* shows the responses to pulses of depolarizing current recorded from the apical dendrite of a layer V cell (Fig. 3*A*) that resembled a corticotectal pyramid (Hübener, Schwarz & Bolz, 1990).

### Isolation of cortical pathways

The two sources of input to layer IV that were investigated during the course of this study were from layer VI and from the thalamus. The contribution of the thalamus to the intralaminar circuit is shown schematically in Fig. 4*A* and the input from layer VI is depicted in Fig. 4*B*; Fig. 4*C* illustrates the convergence of these two ascending paths. Each pathway is drawn only as far away as two synaptic stations from the spiny stellate cell. Layer VI also receives thalamic input but this connection was omitted from the drawing for clarity. The following two experiments show how each pathway was stimulated selectively.

The simplest way to activate the two sources of input separately was to take advantage of the threshold differences between them. Thalamic fibres were activated by electrodes placed in the white matter. Although the white matter contains fibres travelling to and from the cortex, thalamic fibres should be activated by the weakest strength stimulation, since these are thicker than descending ones (McGuire *et al.* 1984; Katz, 1987) and have lower thresholds (Bullier & Henry, 1979; Ferster & Lindström, 1983, 1985; Ferster, 1990). In similar fashion, electrodes placed in layer VI should preferentially activate indigenous elements rather than fibres of passage since cell bodies or their axon hillocks have thresholds lower still than those for axons (Asanuma & Sakata, 1967; Stoney, Thompson & Asanuma, 1968). Also, thalamic axons split into thin branches on entering the white matter (McGuire *et al.* 1984; Freund, Martin, Somogyi & Whitteridge, 1985; Humphrey, Sur, Ulrich & Sherman, 1985) thus sharpening the threshold differences between geniculocortical and endogenous elements in layer VI.

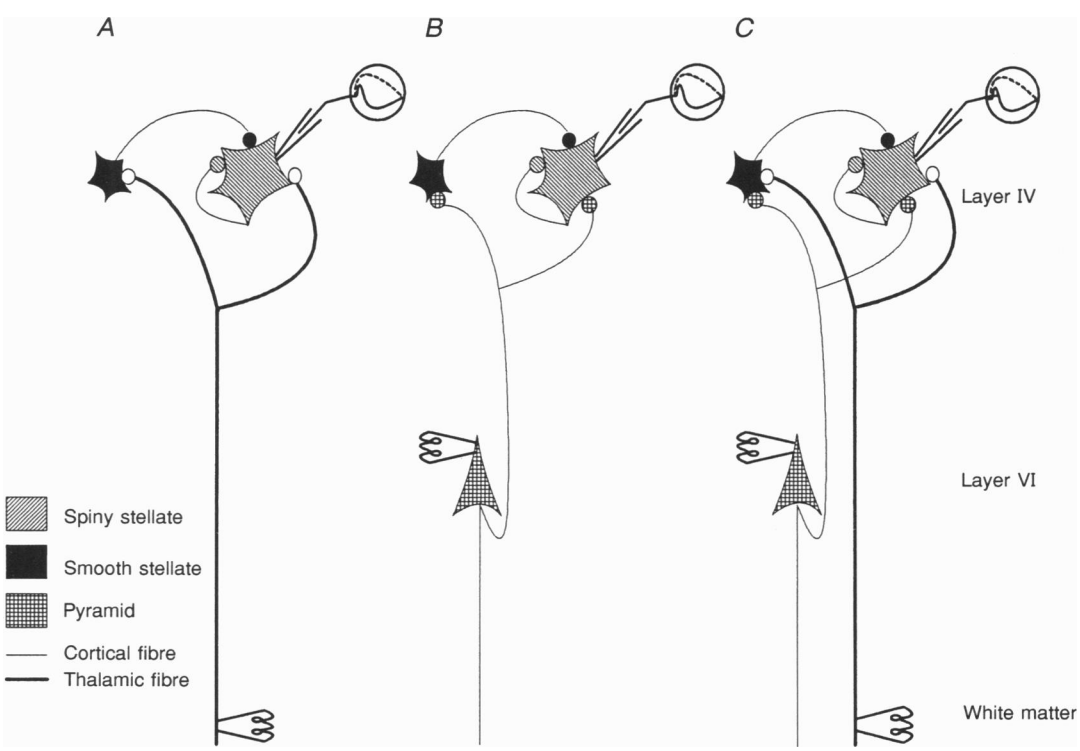


**Figure 4. Schematic diagram of the circuit examined in this study**

The contribution of thalamic input is drawn in *A* and that from layer VI in *B*. The convergence of these pathways is shown in *C*. Each image of a cell represents a population and connections are drawn only as far as two synaptic levels from the spiny stellate cell. Stimulus and recording electrodes are indicated schematically.

Another feature of the anatomy amenable to experimental manipulation is that thalamic afferents are densely packed in the white matter while their branches in the grey matter are scattered in the neuropil. Thus, exciting a small tract of fibres in the white matter can lead to activation of a wide swath of collaterals in the grey matter. The same logic holds for electrode placement in layer VI. Stimulation in the vicinity of the soma, and hence the axonal trunk from which most primary branches emerge (Katz, 1987), should improve the chance of activating entire terminal fields.

Figure 5 provides evidence that inputs from layer VI can be activated in isolation from thalamic fibres. The stimulating electrode was placed on layer VI and a pipette that contained GABA was placed at the stimulus site. Applications of GABA or its agonists are routinely used to inactivate nearby cells while leaving axons of passage

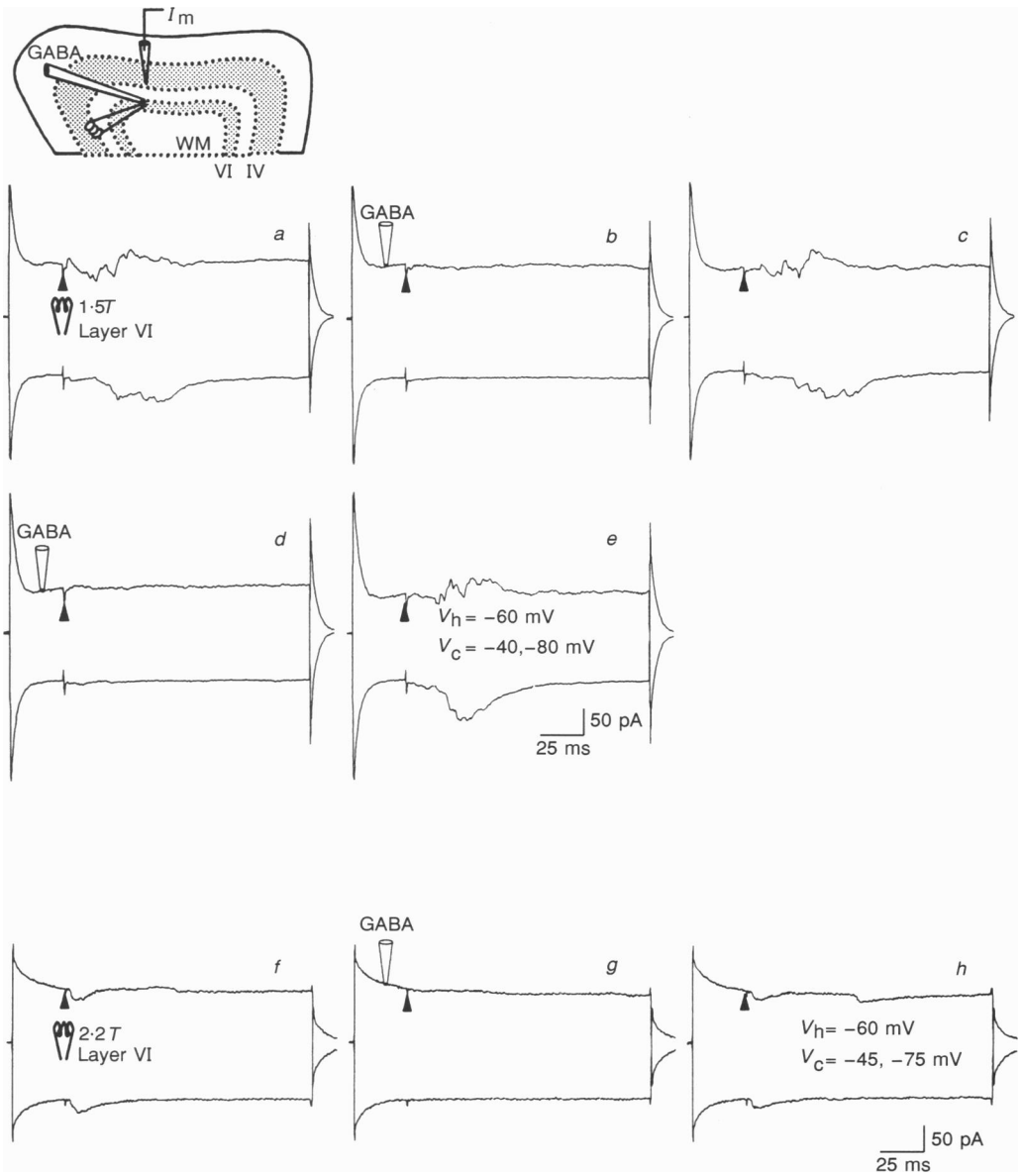


**Figure 5. The synaptic response evoked from layer VI could be reversibly removed by application of GABA**

Here and in subsequent figures, the schematic diagram depicts the preparation. A shock to layer VI was delivered while the command potential ($V_c$) was stepped in equal increments above and below the holding potential ($V_h$) of −60 mV. $I_m$ indicates recording electrode; WM, white matter. Recordings from one cell are shown in *a*–*e*, those from another are in *f*–*h*. For the first cell, panels *b* and *d* show the effects of applying a pulse of GABA (40 mM for 30 ms) several milliseconds before the shock. The resting potential was −60 mV and the input resistance was 222 MΩ. Arrowheads mark the stimulus artifacts. Panels *f* –*h* show control, test and recovery responses, respectively, recorded for the second cell; the resting potential was −60 mV and the input resistance was 190 MΩ.

unaffected, since fibres lack the appropriate receptors (Bolz & Gilbert, 1986; Chapman *et al.* 1991). The recordings were made in the voltage-clamp mode from two different cells in layer IV. Figure 5*a–e* was recorded from one of the cells. It shows the response to a 1·5 threshold ($T$) shock delivered while the membrane was stepped to −40 and then −80 mV from a holding potential of −60 mV. The synaptic response was compound; at −40 mV, both EPSCs and IPSCs were evident (Fig. 5*a*). The synaptic response was suppressed when the shock was applied at the end of the pulse of GABA (Fig. 5*b* and *d*) but returned in full when evoked in the absence of the drug (Fig. 5*c* and *e*). Care was always taken to position the drug pipette downstream, relative to the flow of ACSF, from the recording site. The membrane resistance and the time constant of the patched cells did not change during the application of GABA, as can be seen in the responses to the command steps. Recordings from a second cell for which the monosynaptic EPSC evoked from layer VI was not overlapped by inhibition, are shown in Fig. 5*f–h*. Here again, applying GABA to the stimulus site reversibly eliminated the shock-evoked response. Similar results were obtained from three other cells. The focal inactivation method was effective in demonstrating selectivity only for stimuli in the range of 1–3$T$. This restriction is probably imposed by the degree to which GABA can elevate the threshold for direct activation. For three additional cells tested during separate experiments in which the recording and stimulating electrodes were placed next to each other, local application of GABA elevated the threshold for direct electrical activation only by a factor of two or three (not shown).

Demonstration that thalamic fibres have lower thresholds than descending fibres has come from work *in vivo* (Bullier & Henry, 1979; Ferster & Lindström, 1983, 1985; Ferster, 1990). To provide evidence that this threshold difference is preserved *in vitro*, recordings from five pyramidal cells in layer VI were made (resting potential, −61·7 ± 3·3 mV; input resistance, 168 ± 61 MΩ). The principal ascending input to layer VI is from the thalamus. The threshold voltage required to evoke a synaptic response was found and then stimulus strength was raised to the minimum required for an antidromic spike. Figure 6 illustrates the results from one experiment. Threshold stimuli evoked a small EPSP. The slope and scale of the response increased with shock strength but the synaptic delay remained constant at 3·5 $ms^{-1}$ until an antidromic spike was evoked at 5 times the threshold voltage. The stimulus voltages required for direct activation were 3, 5 and 6$T$ for the three other cells, respectively. A fifth cell could not be activated antidromically.

### Evoked synaptic responses of spiny stellate cells

Postsynaptic potentials evoked by stimulation of layer VI and of the white matter were recorded from thirteen spiny stellate cells. While responses to stimulation of either site varied considerably at stimulus strengths nearer threshold, two general response patterns emerged as the shock voltage was raised to recruit larger portions of the cortical circuit. One class of response was characterized by predominant inhibition and the other by excitation. The synaptic responses evoked for cells ($n = 6$), such as the one in Fig. 7, featured strong inhibition; all recordings shown in this figure were made from a single cell. The selected traces bracket the range of variation that was seen in the subthreshold responses evoked by each stimulus voltage. Postsynaptic events elicited from the white matter are shown in Fig. 7*A*. The threshold response to stimulation of the white matter was an EPSP, the long latency of which showed that it was mediated by more than one synapse.

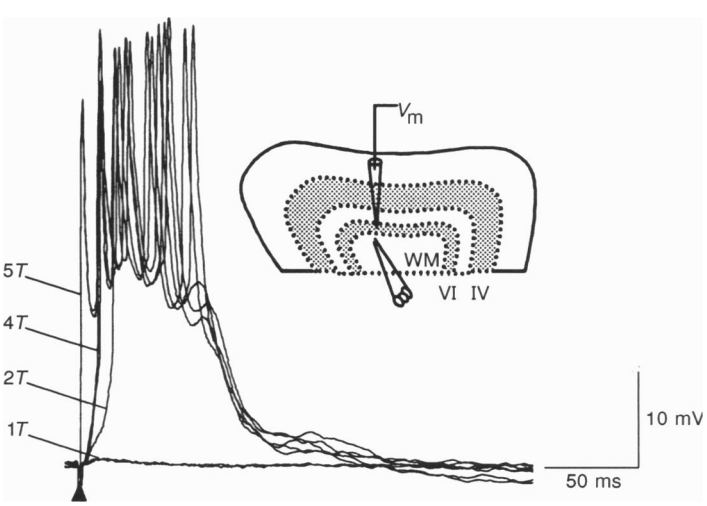


**Figure 6. The threshold for synaptic activation of layer VI pyramids is lower than for antidromic activation**

Superimposed responses of a single cell to 1$T$, 2$T$, 4$T$ and 5$T$ shocks. Two trials for each stimulus are shown. The membrane potential ($V_m$) was −60 mV and the input resistance was 147 MΩ. The arrowhead marks the stimulus artifact.

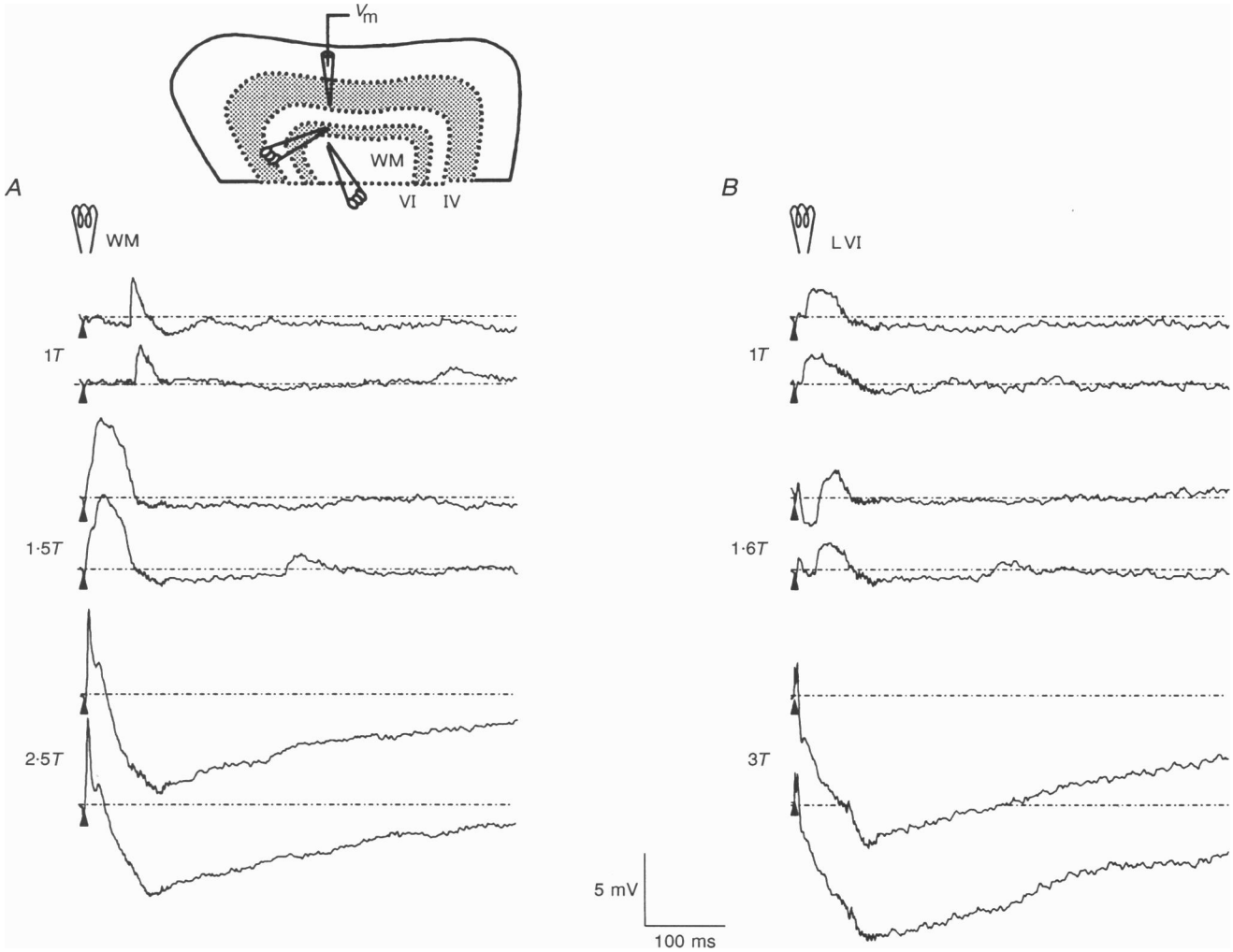


**Figure 7. Synaptic responses evoked from the white matter or from layer VI that featured strong inhibition**

Each set of two traces represents two trials of the same stimulus. Arrowheads mark the stimulus artifacts and the dashed lines denote the resting potential. Shock duration was 100 $\mu$s. The threshold voltage for the white matter was 20 V and was 5 V for layer VI (LVI). The traces in *A* depict low-, medium- and high-strength stimulation of the white matter (1$T$, 1·5$T$, 2·5$T$) and those in *B* illustrate low-, medium- and high-strength stimulation of layer VI (1$T$, 1·6$T$, 3$T$). *C* shows synaptic responses to shocks of 1·75$T$ (top pair) and 2·5$T$ (bottom pair) to the white matter (0·1 Hz) while synaptic input from layer VI was exhausted by delivering 3$T$ shocks (open circles) at 40 Hz; some artifacts were lost in the intersample intervals. The dotted, heavy trace under each pair is the averaged difference between the control responses and those evoked while layer VI was inactivated by rapid stimulation. *D*, the top pair of traces are the responses to a 1·8$T$ shock to layer VI and the middle pair shows the responses to a 1·75$T$ shock to the white matter. Coincident stimulation yielded strong inhibition (bottom pair). The heavy, dotted trace is the difference between the arithmetic sum of the responses evoked by shocking each site alone and the response elicited by coincident activation. All traces in this figure are from the same cell as shown in Fig. 2*A*.

Raising the shock voltage to the range of 1·5–2$T$ to recruit larger numbers of presynaptic fibres, elicited monosynaptic excitation that was accompanied by later EPSPs and a weak prolonged hyperpolarization. Increasing the stimulus strength reversed the sign of the postsynaptic response from largely excitatory to predominantly inhibitory. That is, the most potent stimuli recruited prominent fast and slow IPSPs that eclipsed the EPSPs. The general structure and scale of response remained similar at higher shock voltages (not shown).

As for the white matter, the threshold response from layer VI was conveyed by more than one synapse (Fig. 7*B*, top trace pair). Unlike events initiated in the white matter, even small increments in the shock strength (from 1·2–1·8$T$) evoked prominent IPSPs as well as EPSPs

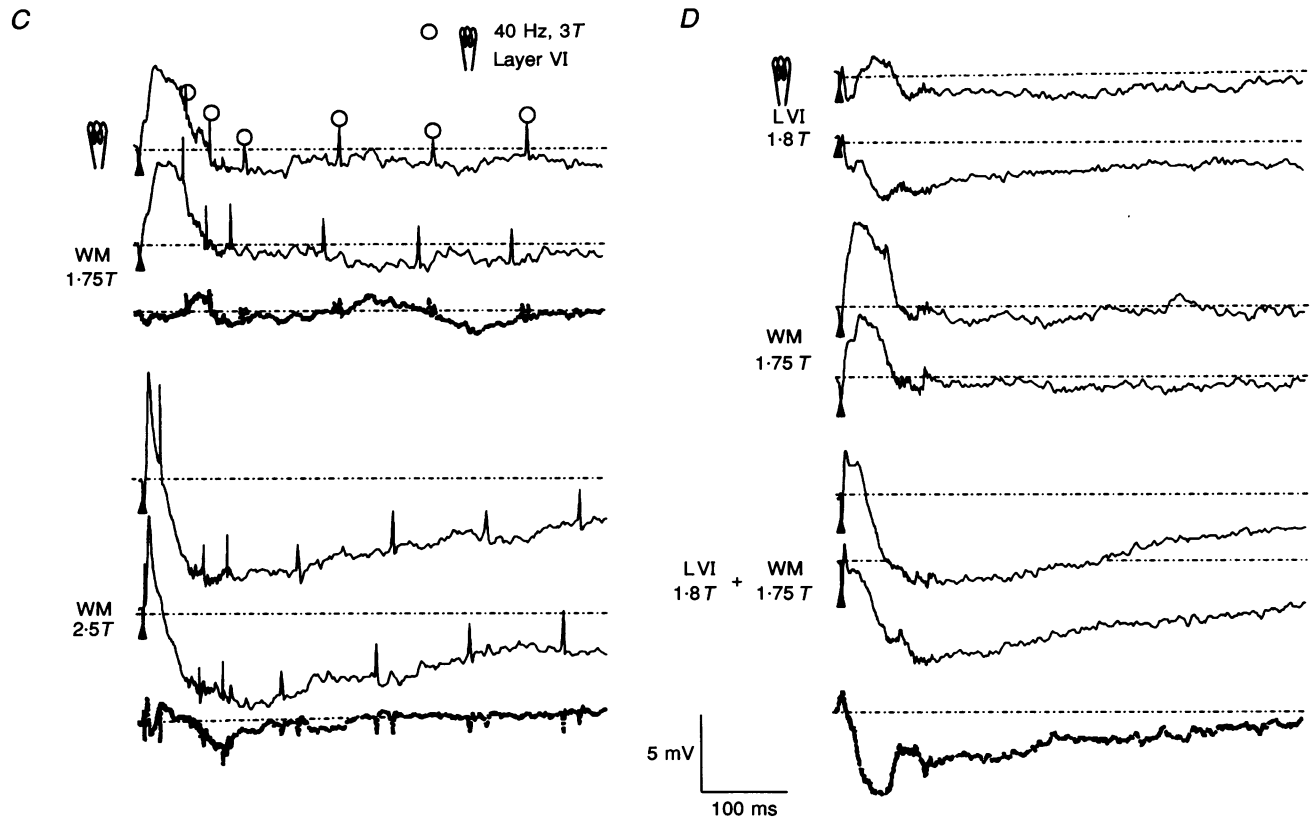


**Figure 7*C* and *D*. For legend, see facing page.**

(Fig. 7*B*, middle trace pair). Stronger shocks evoked a deeply inhibitory response that was far larger in amplitude than that evoked from the white matter (Fig. 7*B*, bottom trace pair).

Certain features of the responses probably reflect general aspects of organization of the cortical circuit and the experimental protocol. If one assumes that weak stimuli are spatially discrete, and may not always reach the cells or fibres that are monosynaptically connected to the patched neuron, it is not surprising that di- or polysynaptic events often comprise the threshold responses. The diverse composition of these responses is in keeping both with the definition of threshold intensity as being effective only a fraction of the time and the likelihood that multiple, synaptic pathways to the patched cell lie near to each other. In addition, integration times at single synaptic stages vary widely (see Fig. 9*C*). The similar response to higher voltages for both sites, however, raised the possibility of stimulus spread.

The experiment illustrated in Fig. 7*C* was designed to test whether or not the responses evoked from the white matter were separate from those evoked directly from layer VI. Responses from the white matter were elicited at the control frequency of stimulation, 0·1 Hz (artifacts marked by arrowheads), while transmission from layer VI was exhausted by stimulation at 40 Hz (artifacts marked by open circles). The stimuli used in this test were 1·75*T* and 2·5*T* shocks to the white matter (the same as those used for the recordings shown in the second pair of traces in Fig. 7*D* and the bottom traces shown in Fig. 7*A*) and 3*T* shocks to layer VI (the same as used for the bottom recordings shown in Fig. 7*B*). The effectiveness of the rapid stimulation procedure was demonstrated by the fact that there were no responses following the shocks to layer VI. (The sampling rate was slowed in the later portions of the traces causing the loss of some artifacts which fell in the gaps between digitized points.) The heavy traces represent the results of subtracting the responses to stimulation of the white matter when the rapid stimuli were being applied, from those collected in the control situation.

Responses to 1·75*T* shocks to the white matter were largely excitatory (Fig. 7*C* top trace pair) and were reduced only slightly, if at all, when inputs from layer VI were fatigued. Some reduction might be expected if part of the response was synaptically relayed through layer VI since this lamina also receives input from the thalamus. The strong inhibitory response evoked by 2·5*T* shocks to the white matter (Fig. 7*C* bottom trace pair) also remained robust when inputs from layer VI were exhausted. Hence, the direct effect of the shocks applied to the white matter was localized to the stimulus site.

For this cell, (Fig. 7*D*), pooling thalamocortical and interlaminar sources had a synergistic inhibitory effect (see the circuit illustrated in Fig. 4*C*). The top traces, which

show mixed EPSPs and IPSPs, were evoked by a 1·8$T$ shock to layer VI. The middle pair of responses are predominantly excitatory and were evoked by a 1·75$T$ stimulus to the white matter. When the postsynaptic response was evoked by activating both the white matter and layer VI together, it was deeply inhibitory. The depth of the inhibition was more profound than that predicted by simply summing the isolated responses. The single heavy trace is the difference between the average of the top four traces subtracted from the average of the bottom pair; thus it represents the portion of the response unaccounted for by linear summation. This additional inhibition was apparently not just the result of a shunt since it remained evident during the later (>100 ms), purely hyperpolarizing phases of the responses.

Records from another cell show that the degree of the synergistic inhibition varies with stimulus conditions (Fig. 8*A*). While the threshold response from layer VI or the white matter was a monosynaptic EPSP, conjoint activation actually reversed the sign of the response and evoked a prominent IPSP (Fig. 8*A*). When the stimulus strength was raised, so that strong inhibition was evoked from both sites and the two IPSPs had similar peak values, concurrent stimulation continued to have a non-linear effect (Fig. 8*B*). For two other spiny stellate cells, coincident activation of both stimulus sites led to responses with peak inhibition, 18 and 40% stronger than predicted by summing the individually evoked postsynaptic events. Thus, four of the six cells that evinced pronounced inhibition also showed non-linear integration of the inputs from the thalamus and layer VI.

The cell featured in Fig. 9 is an example of the type that responded with increasing excitation as larger numbers of inputs were recruited ($n = 4$). A weak shock to the white matter evoked a monosynaptic EPSP (Fig. 9*A*, top trace pair). With an increase in stimulus voltage, that EPSP grew in size (Fig. 9*A*, middle trace pair) and was eventually joined by a later EPSP (Fig. 9*A*, bottom trace pair). At times, slow inhibition following the EPSPs was seen; if fast inhibition was present it was not apparent, perhaps masked by the excitation. The pattern of response evoked from layer VI was more complex. The threshold response was a weak hyperpolarization (Fig. 9*A*, top trace pair). At a slightly higher voltage the synaptic response became more variable. One trial could be overtaken by both fast and slow inhibition while the next was dominated by serial EPSPs. Finally, excitatory events followed by weak and lasting inhibition took precedence in the postsynaptic profile (Fig. 9*B*, bottom trace pair); these responses are reminiscent of responses from the white matter.

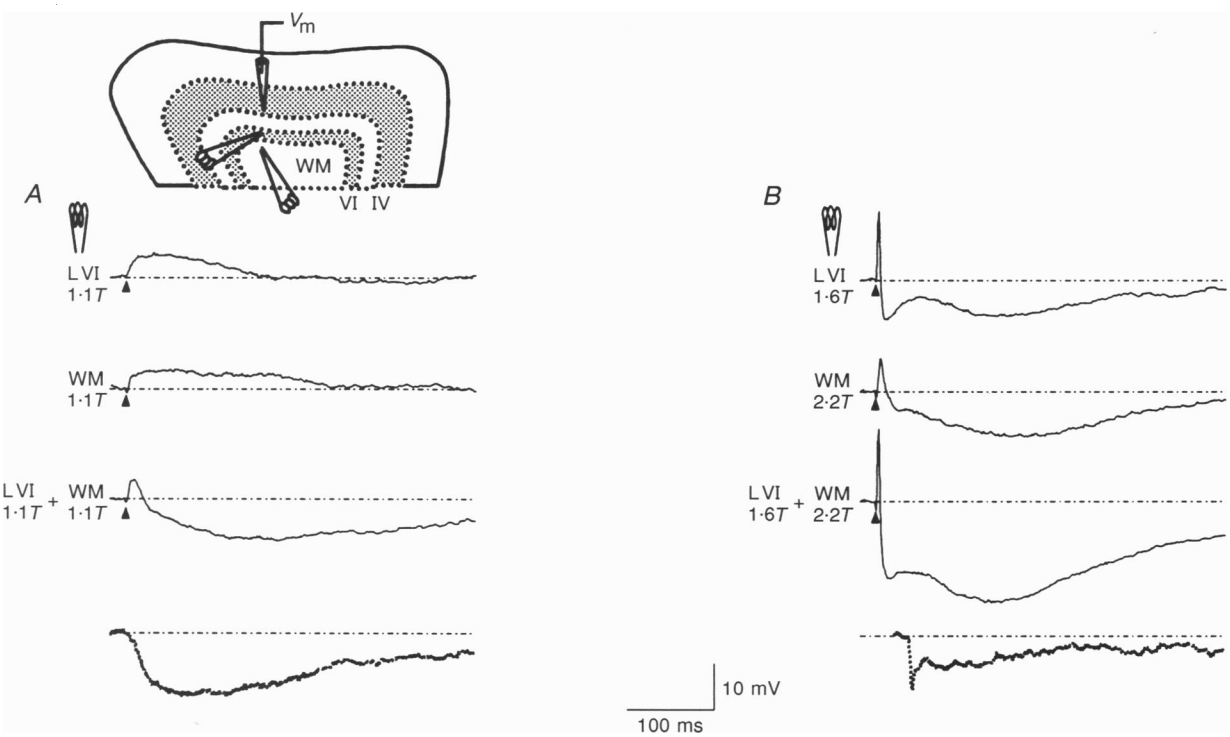


**Figure 8. The strength of the inhibitory interaction varies with stimulus strength**

All traces are the averages of three trials of the same stimulus and were recorded from a single cell. Arrows mark the stimulus artifact. The single dotted heavy trace is the difference between the sum of the responses evoked by shocking each site alone and the response elicited by coincident activation. Shock duration was 100 $\mu$s throughout and stimuli were delivered at 0·1 Hz. The threshold voltage was 11 V for the white matter and 4 V for layer VI. The resting potential was −62 mV and the input resistance was 239 MΩ.

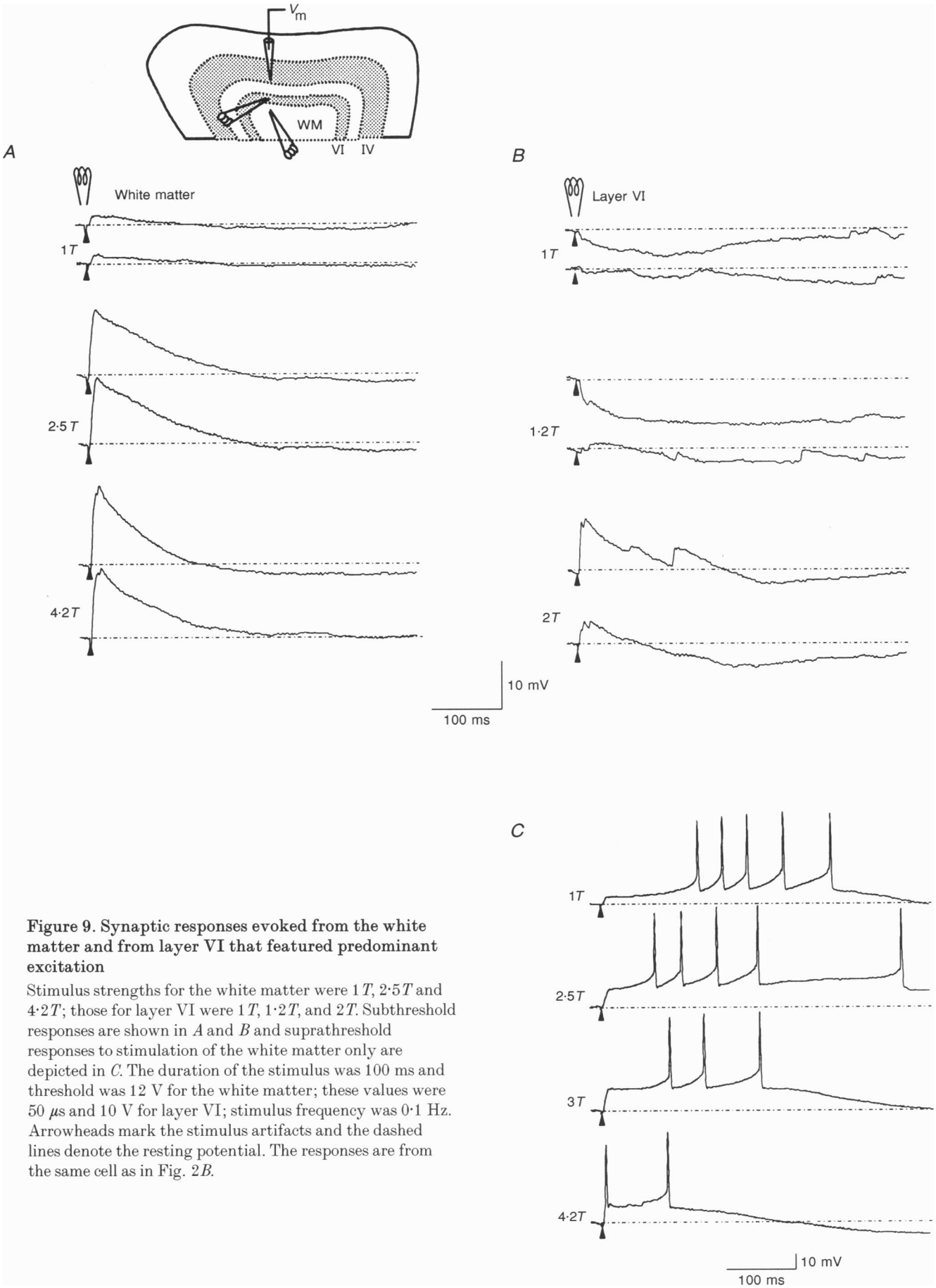


**Figure 9. Synaptic responses evoked from the white matter and from layer VI that featured predominant excitation**

Stimulus strengths for the white matter were 1 *T*, 2·5 *T* and 4·2 *T*; those for layer VI were 1 *T*, 1·2 *T*, and 2 *T*. Subthreshold responses are shown in *A* and *B* and suprathreshold responses to stimulation of the white matter only are depicted in *C*. The duration of the stimulus was 100 ms and threshold was 12 V for the white matter; these values were 50 $\mu$s and 10 V for layer VI; stimulus frequency was 0·1 Hz. Arrowheads mark the stimulus artifacts and the dashed lines denote the resting potential. The responses are from the same cell as in Fig. 2*B*.

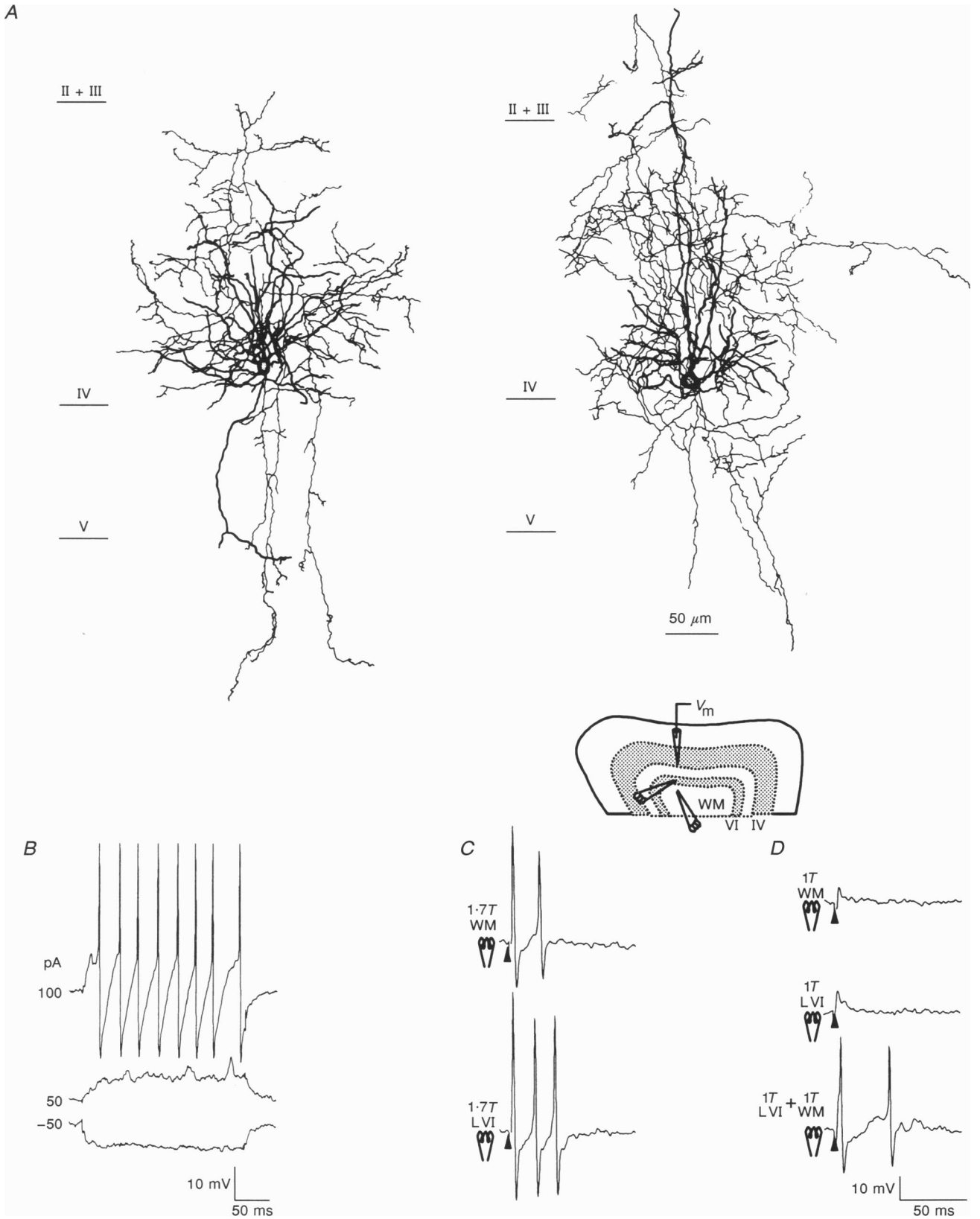


**Figure 10. Morphology and physiology of smooth cells with a fast-spiking pattern**

*A*, a reconstruction of two cells. *B*, responses of the left-hand cell to the injection of current pulses. *C*, responses to 1·7*T* shocks delivered to the white matter (top trace) and layer VI (bottom trace). *D*, subliminal EPSPs evoked from the white matter (top trace) and layer VI (middle trace) and the suprathreshold response elicited by coincident activation of both sites (bottom trace). Arrowheads mark the stimulus artifacts. The membrane potential was −53 mV and the input resistance was 125 MΩ.

In occasional trials the evoked responses were suprathreshold. Figure 9*C* shows examples of the firing evoked by the same stimuli at same membrane potential as in Fig. 9*A*. What is striking about these records is the long integration time of the EPSP at low and intermediate stimulus strengths. Presumably, these long intervals reflect interactions between synaptic inputs and the non-linear properties of the membrane (Staftstrom, Schwindt, Chubb & Crill, 1985; Fig. 2, this paper). The latency tended to decrease as stimulus strength grew, though there could be some fluctuation along the way.

To date, synergistic interactions, such as those shown in Figs 7 and 8, have not been seen in cells with largely excitatory responses. Also, predominantly excitatory patterns were observed in some of the same preparations as the mainly inhibitory ones, indicating that the net sign of the response does not signal poor tissue. For the three remaining cells tested by stimulating both sites, the maximum evoked responses were not clearly weighted towards inhibition or excitation.

### Electrical properties and synaptic responses of smooth stellate cells

The collaterals from layer VI are almost certainly excitatory (McGuire *et al.* 1984; Somogyi, 1989). If they mediate inhibition, they must relay it through inhibitory cells. Recordings made from two classes of smooth cells are shown in Figs 10 and 11 along with anatomical reconstructions of those cells.

Reconstructions of two basket cells are shown in Fig. 10*A*. In each case the soma was located near the bottom of layer IV. The axons arborized extensively within the home layer, suggesting that these cells play a key role in providing intralaminar inhibition. There were also sparse descending projections that extended through layer VI. The left-hand neuron in Fig. 10*A*, in particular, resembles the 'clutch' subtype of basket cell (Kisvárday, Martin, Whitteridge & Somogyi, 1985). Recordings from that cell are shown in Fig. 10*B*, *C* and *D* and are representative of both. Depolarizing pulses of current evoked brief action potentials (<0·5 ms at half-height) the frequency of which did not adapt with time (Fig. 10*B*).

Stimuli applied to the white matter or to layer VI could excite the cell strongly at stimulus strengths above threshold (Fig. 10*C*). Impressively, the small EPSPs evoked by weak shocks to one stimulus site or the other, summed to produce serial action potentials when both pathways were activated in synchrony (Fig. 10*D*).

Two examples of a different physiological type of smooth cell are pictured in Fig. 11*A*. Each of these had its soma in the middle of layer IV; the axonal arborization was mainly in layer IV and lacked projections to layer VI ($n = 3$). These cells had action potentials with half-heights of >0·5 ms and rates showing adaptation over time (Fig. 11*B*). The recordings shown here were made from the cell pictured to the right in Fig. 11*A*. The synaptic response to stimulation of the white matter differed from that evoked from layer VI (Fig. 11*C*, top trace). Shocks applied to the white matter evoked a weak EPSP followed by an IPSP (Fig. 11*C*, top trace). The top trace was recorded while the membrane was several millivolts more depolarized than when the other traces were obtained. The postsynaptic events following activation of layer VI had a nearly reciprocal pattern. The postsynaptic response to intracortical stimulation was a burst of action potentials (Fig. 11*C*, bottom trace). The recording ended before simultaneous activation of the pathways could be tested. The two additional neurons were each activated from one site only. One neuron was strongly excited by input from layer VI and the other had a largely inhibitory response to activation of the white matter.

## DISCUSSION

The focus of this study was to learn about how patterns of synaptic integration in layer IV might contribute to the generation of cortical response properties. Recordings were made from spiny stellate cells and from two physiologically distinct classes of basket cell. Stimulation of the white matter or layer VI led to various balances of multisynaptic excitation and inhibition in spiny stellate cells. In some instances, activating both pathways together yielded stronger inhibition than was predicted from simply adding the responses evoked by each pathway alone. Records of the synaptic responses of smooth cells gave insight into the structure of underlying inhibitory circuits.

### Intrinsic properties of cells in the layer IV microcircuit

The results show that spiny stellate cells fired trains of fast, regular action potentials, the rate of which slowed with prolonged depolarization. The current–voltage relationships were non-linear; steeper above the resting potential than below it. Thus, to a first approximation, the electrical behaviour of spiny stellate cells resembles that of most types of pyramidal cell (Staftstrom *et al.* 1985; Spain, Schwind & Crill, 1987; Hirsch & Gilbert, 1991). Earlier reports have described bursting firing patterns in layer IV (Chagnac-Amitai & Connors, 1989). Although it has been shown here and by Amitai, Friedman, Connors & Gutnick (1993) that such recordings could easily have resulted from the impalement of the apical dendrites of lower layer pyramids, it is possible that a subpopulation of bursting spiny stellate cells escaped notice.

Two types of basket cells in layer IV were distinguished by their firing properties. One variety, the fast-spiking basket cell, is familiar, and was originally described in the neocortex by McCormick, Connors, Lighthall & Prince (1985) and specifically in layer IV by Stern, Edwards & Sakmann (1992). Numerous anatomical populations of smooth cells seem to share this spiking pattern (McCormick *et al.* 1985). The second kind of basket cell had slower action potentials and firing rates that showed frequency

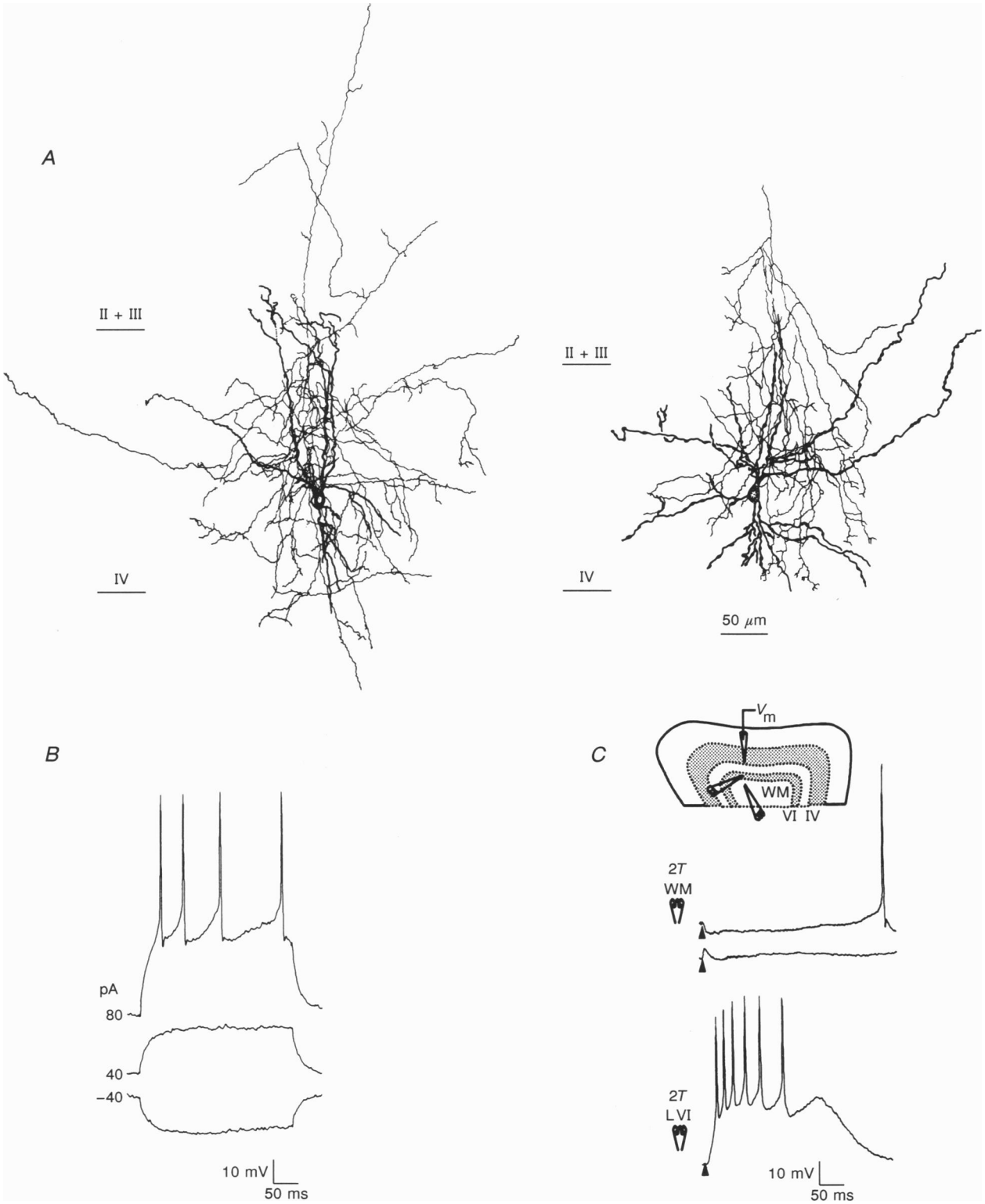


**Figure 11. Morphology and physiology of smooth cells with an adapting firing pattern**

*A*, reconstruction of two cells. *B*, responses of the right-hand cell to the injection of current pulses. *C*, top trace, responses to a 2*T* shock to white matter. The membrane potential in the upper trace was about 3 mV more depolarized than in the others; bottom trace, response to a 2*T* shock to layer VI. Arrowheads mark the stimulus artifacts. The resting potential was −57 mV and the input resistance was 214 MΩ.

adaptation. Inhibitory cells with slow, adapting action potentials that fire in bursts, were first described in the hippocampus by Miles & Wong (1984) and have been found in agranular cortex by Kawaguchi (1993). It is not yet clear how many morphological classes have this physiology.

**Synaptic mechanisms**

A variety of neuronal response properties are suppressive, with end-inhibition being a well-studied example (Hubel & Wiesel, 1965; Berman, Douglas, Martin & Whitteridge, 1991). About half of the cells in layer IV are end-stopped; increasing the length of the stimulus beyond the optimum causes a progressive reduction in firing rate (Hubel & Wiesel, 1962; Dreher, 1972; Gilbert 1977; LeVay *et al.* 1987). The ascending interlaminar projection could be one route for conveying end-inhibition (cf. Sherk & LeVay, 1981), presumably via a disynaptic inhibitory loop (McGuire *et al.* 1984). Firstly, the receptive fields in layer VI are often longer than those in layer IV (Gilbert, 1977) and, importantly, are rarely end-stopped themselves (Gilbert, 1977; Grieve & Sillito, 1991). Additionally, the axonal arbors of layer VI cells are densely and widely distributed in layer IV (McGuire *et al.* 1984; Katz, 1987). Furthermore, Bolz & Gilbert (1986) demonstrated that inactivation of layer VI reduced end-stopping in layer IV. Lastly, Martin *et al.* (1983) have identified a smooth cell in cat layer IV that showed length summation.

The pathway from layer VI to layer IV has diverse functional effects. By selectively activating cortico-geniculate fibres, Ferster & Lindström (1983, 1985) demonstrated directly that the ascending interlaminar pathway has a strongly excitatory action. Studies by Grieve & Sillito (1992) suggest that input from layer VI may increase overall activity in some layer IV cells.

*In vitro*, spiny stellate cells tended to be divided into two groups defined by the net sign of the response that followed strong activation of ascending inputs. For about half the cells, the balance of the PSP was inhibitory and for the other half, excitatory. Probably, the di- and poly-synaptic components of the response were conveyed mainly by terminals of neurons in layers IV and VI. A large contribution from layers II + III and V is unlikely, since the cortical circuit directs information from these through layer VI (Gilbert & Kelly, 1975; Lund *et al.* 1979). Conceivably, *in vitro*, cells that responded with dominant inhibition to high stimulus strength correspond to the end-stopped population *in vivo*.

Striking results came from the spiny stellate cells that responded to strong stimulation with predominant inhibition. When relatively weak shocks were used to drive selectively inputs both from the white matter and layer VI, there were instances where concurrent activation of both pathways suppressed excitation from the thalamus and had a net hyperpolarizing effect that was far larger than the one predicted by summing the responses evoked by either path alone. Such patterns of synaptic integration may underlie suppressive interactions like end-inhibition *in vivo*.

One simple explanation of the synergy between pathways is as follows. Some smooth cells that receive input from the thalamus and layer VI may be most effective when driven by both sources, at least under stimulus conditions when one pathway is too weakly activated to exert substantial influence by itself. Evidence for this type of circuitry was provided by recordings made from fast-spiking basket cells (Fig. 10).

In contrast to the pattern of convergent excitation, inhibitory mechanisms could take the form of a push–pull relationship between afferent pathways. An example is the adapting basket cell illustrated in Fig. 11. At intermediate stimulus range, the net effect of thalamic input was inhibitory but the response from layer VI was excitatory. *In vivo*, the suppressive effects of such circuits might be felt most deeply when stimulus conditions favour activation of cells in layer VI.

Lastly, it is likely that the inhibitory effects directly conveyed from smooth to spiny stellate cells would be indirectly enhanced by a consequential withdrawal of local excitatory drive. That is, preventing activity in one spiny stellate cell would check the effects of that cell on its postsynaptic targets and their neighbours in turn. This possibility remains to be tested in experiments detailing the intralaminar circuitry.

All told, the idea that non-linear inhibitory interactions arise through synaptic vetoes underlain by shunting inhibition has been cast into doubt by the failure to detect any such process *in vivo* (Douglas, Martin & Whitteridge, 1988; Berman *et al.* 1991; Ferster & Jagadeesh, 1992). The results presented here provide evidence that grouped action of components of the cortical circuit can, in fact, generate strongly non-linear inhibition.

Amitai, Y., Friedman, A., Connors, B. W. & Gutnick, M. J. (1993). Regenerative activity in apical dendrites of pyramidal cells in rat neocortex. *Cerebral Cortex* **3**, 26–38.

Asanuma, H. & Sakata, H. (1967). Functional organization of a cortical efferent system examined with focal depth stimulation in cats. *Journal of Neurophysiology* **30**, 35–54.

Berman, N. J., Douglas, R. J., Martin, K. A. C. & Whitteridge, D. (1991). Mechanisms of inhibition in cat visual cortex. *Journal of Physiology* **440**, 697–722.

Blanton, M., LoTurco, J. J. & Kriegstein, A. R. (1989). Whole-cell recording from neurons in slices of reptilian and mammalian cerebral cortex. *Journal of Neuroscience Methods* **30**, 203–210.

Bolz, J. & Gilbert, C. D. (1986). Generation of end-inhibition in the visual cortex via interlaminar connections. *Nature* **320**, 362–365.

BULLIER, J. & HENRY, G. H. (1979). Laminar distributions of first order neurons and afferent terminals in cat striate cortex. *Journal of Neurophysiology* **42**, 1271–1281.

CHAGNAC-AMATAI, Y. & CONNORS, B. W. (1989). Synchronized excitation and inhibition driven by intrinsically bursting neurons in neocortex. *Journal of Neurophysiology* **62**, 1149–1162.

CHAPMAN, B. & STRYKER, M. P. (1993). Activity-dependent development of orientation specificity in ferret primary visual cortex. *Journal of Neuroscience* **13**, 5251–5262.

CHAPMAN, B., ZAHS, K. R. & STRYKER, M. P. (1991). Relation of cortical cell orientation selectivity to alignment of receptive fields of the geniculocortical afferents that arborize within a single orientation column in ferret visual cortex. *Journal of Neuroscience* **11**, 1347–1358.

DOUGLAS, R. J., MARTIN, K. A. C. & WHITTERIDGE, D. (1988). Selective responses of visual cortical cells do not depend on shunting inhibition. *Nature* **332**, 642–644.

DREHER, B. (1972). Hypercomplex cells in the cat's striate cortex. *Investigative Ophthalmology and Visual Science* **11**, 355–356.

EDWARDS, F. A, KONNERTH, A., SAKMANN, B. & TAKAHASHI, T. (1989). A thin slice preparation for patch clamp recordings from neurons of the mammalian central nervous system. *Pflügers Archiv* **414**, 600–612.

FERSTER, D. (1990). X- and Y-mediated synaptic potentials in neurons of areas 17 and 18 of cat visual cortex. *Visual Neuroscience* **4**, 115–133.

FERSTER, D. & JAGADEESH, B. (1992). EPSP–IPSP interactions in cat visual cortex studied with *in vivo* whole-cell patch recording. *Journal of Neuroscience* **14**, 1262–1274.

FERSTER, D. & LINDSTRÖM, S. (1983). An intracellular analysis of geniculo-cortical connectivity in area 17 of the cat. *Journal of Physiology* **342**, 181–215.

FERSTER, D. & LINDSTRÖM, S. (1985). Synaptic excitation of neurons in area 17 of the cat by intracortical axon collaterals of cortico-geniculate cells. *Journal of Physiology* **367**, 233–252.

FREUND, T. F., MARTIN, K. A. C., SOMOGYI, P. & WHITTERIDGE, D. (1985). Innervation of cat visual areas 17 and 18 by physiologically identified X- and Y-type thalamic afferents. I. Arborization patterns and quantitative distribution of postsynaptic elements of postsynaptic targets by GABA immunocytochemistry and Golgi impregnation. *Journal of Comparative Neurology* **242**, 263–273.

GILBERT, C. D. (1977). Laminar differences in receptive field properties of cells in cat primary visual cortex. *Journal of Physiology* **268**, 391–421.

GRIEVE, K. L. & SILLITO, A. M. (1991). A reappraisal of the role of layer VI of the visual cortex in the generation of cortical end inhibition. *Experimental Brain Research* **87**, 521–529.

HAMILL, O. P., MARTY, A., NEHER, E., SAKMANN, B. & SIGWORTH, F. J. (1981). Improved patch clamp technique for high resolution current recording from cells and cell free patches. *Pflügers Archiv* **391**, 85–100.

HIRSCH, J. A. (1992). The first stage of visual processing. *Society for Neuroscience Abstracts* **18**, 209.

HIRSCH, J. A. & GILBERT, C. D. (1991). Synaptic physiology of horizontal connections in the cat's visual cortex. *Journal of Neuroscience* **11**, 1800–1809.

HORIKAWA, K. & ARMSTRONG, W. E. (1988). A versatile means of labeling: injection of biocytin and its detection with avidin conjugates. *Journal of Neuroscience Methods* **25**, 1–11.

HUBEL, D. H. & WIESEL, T. N. (1962). Receptive field, binocular interaction and functional architecture in the cat's visual cortex. *Journal of Physiology* **160**, 106–154.

HUBEL, D. H. & WIESEL, T. N. (1965). Receptive fields and functional architecture in two nonstriate visual areas 18 and 19 of the cat. *Journal of Neurophysiology* **28**, 229–289.

HÜBENER, M., SCHWARZ, C. & BOLZ, J. (1990). Morphological types of projection neurons in layer 5 of cat visual cortex. *Journal of Comparative Neurology* **301**, 655–674.

HUMPHREY, A. L., SUR, M., ULRICH, D. J. & SHERMAN, S. M. (1985). Projection patterns of individual X- and Y-cell axons from the lateral geniculate nucleus to cortical area 17 in the cat. *Journal of Comparative Neurology* **233**, 159–189.

KATZ, L. C. (1987). Local circuitry of identified projection neurons in cat visual cortex brain slices. *Journal of Neuroscience* **7**, 1223–1249.

KAWAGUCHI, Y. (1993). Groupings of nonpyramidal and pyramidal cells with specific physiological and morphological characteristics in rat frontal cortex. *Journal of Neurophysiology* **69**, 416–431.

KISVÁRDAY, Z. F., MARTIN, K. A. C., WHITTERIDGE, D. & SOMOGYI, P. (1985). Synaptic connection of intracellularly filled clutch cells: A type of small basket cell in the visual cortex of the cat. *Journal of Comparative Neurology* **241**, 111–137.

LEVAY, S., MCCONNELL, S. K. & LUSKIN, M. B. (1987). Functional organization of primary visual cortex in the mink (*Mustela vison*) and a comparison with the cat. *Journal of Comparative Neurology* **257**, 422–441.

LORENTE DE NÓ, R. (1944). Cerebral cortex: Architecture, intracortical connections, motor projections. In *Physiology of the Nervous System*, ed. FULTON, J. F., pp. 291–325. Oxford University Press, London.

LUND, J. S., HENRY, G. H., MACQUEEN, C. L. & HARVEY, A. R. (1979). Anatomical organization of the primary visual cortex (area 17) of the cat. A comparison with area 17 of the macaque monkey. *Journal of Comparative Neurology* **184**, 599–618.

MCCORMICK, D. A., CONNORS, B. W., LIGHTHALL, J. W. & PRINCE, D. A. (1985). Comparative electrophysiology of pyramidal and sparsely spiny stellate neurons. *Journal of Neurophysiology* **54**, 782–806.

MCGUIRE, B., HORNUNG, J. P., GILBERT, C. D. & WIESEL, T. N. (1984). Patterns of synaptic input of layer IV of the cat striate cortex. *Journal of Neuroscience* **4**, 3021–3033.

MARTIN, K. A. C. SOMOGYI, P. & WHITTERIDGE, D. (1983). Physiological and morphological properties of identified basket cells in the cat's visual cortex. *Experimental Brain Research* **50**, 193–200.

MILES, R. & WONG, R. K. S. (1984). Unitary inhibitory synaptic potentials in the guinea-pig hippocampus *in vitro*. *Journal of Physiology* **356**, 97–113.

SAINT MARIE, R. L. & PETERS, A. (1985). The morphology and synaptic connections of spiny stellate neurons in monkey visual cortex (area 17): A Golgi-electron microscopic study. *Journal of Comparative Neurology* **233**, 213–235.

SHERK, H. & LEVAY, S. (1981). The visual claustrum of the cat. III. Receptive field properties. *Journal of Neuroscience* **1**, 993–1002.

SOMOGYI, P. (1989). Synaptic organization of GABAergic neurones and $GABA_A$ receptors in the lateral geniculate nucleus and visual cortex. In *Neural Mechanisms of Visual Perception*, ed. LAM, D. M. & GILBERT, C. D., pp. 35–62. Gulf Publishing Co., Houston,USA.

SPAIN, W. J., SCHWINDT, P. C. & CRILL, W. E. (1987). Anomalous rectification in neurons from cat sensorimotor cortex *in vitro*. *Journal of Neurophysiology* **57**, 1555–1576.

STAFTSTROM, C. E., SCHWINDT, P. C., CHUBB, M. C. & CRILL, W. E. (1985). Properties of persistent sodium conductance and calcium conductance of layer V neurons from cat somatosensory cortex *in vitro*. *Journal of Neurophysiology* **53**, 1153–1170.

STERN, P., EDWARDS, F. A. & SAKMANN, B. (1992). Fast and slow components of unitary EPSCs on stellate cells elicited by focal stimulation in slices of the rat visual cortex. *Journal of Physiology* **449**, 247–278.

STONEY, S. D., THOMPSON, W. D. & ASANUMA, H. (1968). Excitation of pyramidal tract cells by intracortical microstimulation: effective extent of stimulating current. *Journal of Neurophysiology* **31**, 659–669.

**Acknowledgements**

T. N. Wiesel provided support and advice during all phases of the project. R. C. Reid and M. V. Sánchez-Vives made careful comments about the manuscript. J. K. Carrol and C. A. Gallagher assisted with histological procedures and C. A. Gallagher drew the labelled cells. P. R. Peirce patiently photographed the drawings. K. Christian provided advice about computers. This work was funded by NIH grant EYO9593 and a Klingenstein Award to J. A. H. and by NIH grant EYO5253 to T. N. W.

*Received 21 February 1994; accepted 22 August 1994.*